Iron chelation by deferoxamine as useful adjunct therapeutics in murine tuberculosis.

Sandeep R. Kaushik,[1] Sukanya Sahu,[1] Amit Kumar Mohapatra,[1] Nidhi Yadav,[1] Adyasha Sarangi,[1] Swati Kumari,[2] Bichitra Biswal,[2] Ranjan Kumar Nanda[1,*]

[1]Translational Health Group, International Centre for Genetic Engineering and Biotechnology, New Delhi- 110067, India.

[2]Structural and Functional Biology Laboratory, National Institute of Immunology, New Delhi-110067, India.

Short title: Altered iron homeostasis in tuberculosis patients

***Corresponding author**

Ranjan Kumar Nanda (PhD)

Translational Health Group, International Centre for Genetic Engineering and Technology, New Delhi-110067, India

Telephone: 91-11-26741358; E mail: ranjan@icgeb.res.in

Abstract: Iron is a critical element used for survival of both host and pathogens. Tuberculosis patients show dysregulated iron metabolism and provide an opportunity for developing host directed therapeutics. In this study, C57BL/6 mice supplemented with ferric carboxymaltose and controls were aerosol infected with 100-120 CFU of the H37Rv strain of *Mycobacterium tuberculosis.* A subgroup of mice received deferoxamine (DFO) with or without isoniazid and rifampicin. The iron supplemented C57BL/6 mice showed higher tissue mycobacterial burden at 2 weeks of post infection. The efficacy of isoniazid and rifampicin was compromised in iron supplemented C57BL/6 mice. Iron chelation by deferoxamine (DFO) alone for a month significantly reduced the tissue mycobacterial burden but was less effective in the iron-supplemented group. DFO as an adjunct to isoniazid and rifampicin cleared the tissue mycobacteria more efficiently. Currently, DFO is used for treating acute iron poisoning and iron overloaded thalassemic patients and holds promise as an adjunct therapeutic agent for TB.

Keywords: Tuberculosis, Iron overloading, Iron chelation, Deferoxamine, Host directed therapeutics.

Introduction: Tuberculosis (TB) is caused by the infection of *Mycobacterium tuberculosis* (Mtb) and affects multiple tissues including lungs.[1] The treatment duration modalities for TB patients infected with drug sensitive Mtb strains is 6-9 months and may take up to 24 months or more if infected with drug resistance strains.[2] Shortening the treatment duration with additional host directed therapeutics (HDT) might reduce the relapse rate, minimize drug resistance development and millions of life lost every year due to TB.[3]

Iron supplementation in TB patients reported to worsen clinical outcome.[4,5,6,7] Whereas, iron chelation, in *in-vitro* and *in-vivo* settings significantly reduces Mtb load.[8] In this study, the impact of iron supplementation and iron chelation on the mycobacterial burden of C57BL/6 murine model was monitored. We report that FDA approved iron chelating agents like deferoxamine (DFO) has mycobactericidal properties and with TB drugs accelerate Mtb clearance in C57BL/6 mice.[9] DFO as an adjunct therapy in TB may be useful to reduce the treatment duration and need additional clinical studies to understand its clinical utility.

Methodology

Ethical statement: The experiments adopted in this study were approved by the Institute Biosafety Committee and the Institute Animal Ethics Committee (ICGEB/IAEC/07032020/TH-11) of International Center for Genetic Engineering and Biotechnology New Delhi.

Mycobacterial H37Rv culture: *Mycobacterium tuberculosis* H37Rv strain (OD=0.02) were inoculated to 7H9 media (BD Difco Middlebrook) supplemented with Glycerol (0.005%), tween 80 (0.05%) and OADC (Oleate Albumin Dextrose and catalase, 10%) in the absence or presence of individual drugs alone or in combination in the tuberculosis aerosol challenge facility (TACF, BSL-III) at ICGEB New Delhi. Mtb were grown in a shaker incubator set at 180 rpm at 37°C. Individual drug solutions were prepared at their minimum inhibitory concentrations (MICs) i.e. DFO (0.1 mg/ml) and isoniazid (0.1 µg/ml) prepared using milliQ

water. Mtb growth was monitored by measuring absorbance at 600 nm upto 5 days post inoculation using a spectrophotometer to monitor their bactericidal activity at an interval of 24 hours. On the fifth day, the harvested control and drug-treated Mtb were inoculated on 7H11 plates for colony forming unit (CFU) assay. At the fifth day, a fraction of the Mtb culture (~0.8×10^8) were centrifuged at 4000 rpm for 10 minutes at room temperature to harvest the Mtb and media fraction for elemental analysis using inductively coupled plasma mass spectrometry (ICP-MS) analysis.

Elemental analysis of the bacterial cells and culture filtrate using ICP-MS: To the harvested Mtb pellet, HNO_3 (70%, 150 µl) was added and after transferring to sample vials (MG5, Anton Paar, USA) H_2O_2 (30%, 50 µl) was added. Similarly, to the culture filtrates (~1 ml), HNO_3 (70%, 500 µl) and H_2O_2 (30%, 150 µl) were added. The sealed sample vials were subjected to microwave (Anton Paar, USA) digestion using a ramp of 250W for 15 min with a hold time for 5 min at 250W.

After appropriate dilution with trace metal-free water, iron (57Fe), copper (63Cu), zinc (66Zn) levels were monitored in the digested samples using ICP-MS (iCAPTM TQ ICP-MS, Thermo Scientific, USA). Thermo Scientific Qtegra Intelligent Scientific Data Solution (ISDS) software was used for operating and controlling the instrument. Following the manufacturer's instruction, calibration plot for 57Fe, 63Cu, 66Zn (0.1 ppb to 1 ppm) was prepared using the multi-element standard mix (#92091, Sigma Aldrich). Briefly, digested samples were aspirated using sample capillary (0.55 mm) through a V grooved Micromist DC nebulizer and spray chamber of ICP-MS. Samples were passed through a quartz torch, with an injector diameter of 2 mm, which produces plasma. Samples were ionized by plasma and passed through sample cones followed by a skimmer cone. To avoid any polyatomic ion interference, data acquisition was carried out using KED (Kinetic energy dissociation) mode. The nebulizer flow was set at 1.045 l/min with a pressure of 3.20 bar, the peristaltic pump was revolving clockwise (40 rpm)

and instrument exhaust was maintained at 0.47 mbar. Interface temperature was maintained at 30.53°C with a cool flow of 14 l/min. Nickel sample and skimmer cones with orifice's diameter of 1 mm and 0.5 mm respectively were used. To remove carryover between sample runs if any, HNO_3 (1%) was pumped through the nebulizer with a wash-out time of 30 sec. During the sample run, a dwell time of 0.1s was followed. The average value from the three runs were used to calculate the 57Fe levels and exported for further statistical analysis.

Atomic structure analysis of the iron storage proteins in Mycobacterium tuberculosis: The atomic coordinates of the 3D structures of known iron storage proteins in Mtb i.e. both BfrA (Rv1876) and BfrB (Rv3841) were obtained from the Protein Data Bank (www.rcsb.org).[10, 11, 12] The 3D structures of BfrA and BfrB were analyzed and figures were made using Pymol molecular visualization software.[13]

Iron supplementation in C57BL/6 mice and aerosol Mtb infection: C57BL/6 mice (8-10 weeks old, male) from the ICGEB animal house were transferred to the TACF for adaptation for at least one week prior to the infection experiment. The animals were kept in a specific pathogen free environment, 12-hours daylight conditions, food and water were provided *ad-libitum*. A set of the study mice received ferric-carboxymaltose (Ferinject, LUPIN ltd, India, 0.5 mg iron/mice in 100 µl saline) through intravenous injection, while the control mice received saline (100 µl). These iron supplemented mice received a total of four doses of ferric-carboxymaltose injections on every fourth day. After a week of rest the iron supplemented and control mice were aerosol infected with a low dose (110-120 CFU) of Mtb H37Rv strain using Madison chamber in TACF and sacrificed at 1, 15, 45- and 90-days post infection to monitor for tissue bacterial load. Briefly, mice were anesthetized using 5% Isoflurane and organs were harvested from the humanely euthanized mice. Whole blood (˜500 µl) was collected from the study animals just before euthanization by cardiac puncture. Serum was collected after incubating for 30 min at room temperature followed by centrifugation at 1500 rpm for 10 min

at 4ºC and stored immediately at -80ºC until used. Harvested tissues (lungs, spleen, liver) were homogenized using a homogenizer at 10-12,000 rpm in 1 ml of sterile PBS. A part of it (100 µl) was inoculated on 7H11 agar plates at appropriate dilution in sterile PBS and the colonies were counted post 3 weeks of incubation at 37ºC in the incubator. A part of whole blood and tissues were stored at -80 ºC for elemental analysis using ICP-MS.

Anti-TB treatment and Colony-forming unit (CFU) assays: A sub group of Mtb infected C57BL/6 mice received either Isoniazid-Rifampicin (IR) or Deferoxamine (DFO: D) or both (IRD) from 15 days post infection till 90 days. DFO (150 mg/Kg body weight of mice) was introduced intraperitoneally every fourth day till treatment completion. Isoniazid and Rifampicin (0.1 g/l) were provided in drinking water ad-libitum and changed every alternate day. The IRD group received the same dose of both IR and DFO and the control Mtb infected group did not receive any drugs. Multiple tissue (lungs, liver, and spleen) bacterial loads at day 1, 15, 45- and 90-days post infection were monitored by CFU assay, explained in the earlier section. A part of the tissue of these C57BL/6 mice were stored for elemental analysis using ICP-MS.

Histology slides preparation: A part of the harvested tissues were stored in 10% formaldehyde for histology analysis. Briefly, processed tissues were paraffin embedded and 5 µm thickness sections were used for slide preparation at a pathology lab. Prussian blue staining was used for monitoring tissue iron distribution.

Blood and liver iron estimation using ICPMS: Whole blood samples (˜50 µl) or liver tissue samples (˜50 mg) were taken in a digestion vial (64MG5 vials). HNO_3 (400 µl) and H_2O_2 (100 µl) were added to the vials followed by 20 min incubation at room temperature, and then the vials were sealed. The sealed vials were capped and placed in an Anton-Paar Multiwave Pro microwave digester for sample digestion. The initial power was set at a ramp of 10 min and 150 watt in with a max temperature of 140ºC, followed by a 15 min hold. Then a second ramp

of 15 min from 150-250 watt used and a final hold to bring the temperature to 55°C at highest fan speed. The digested samples were cooled down further at room temperature before puncturing the cap of vials. Briefly, acid-digested blood and tissue samples were diluted with ddH_2O before acquiring data using ICPMS (Triple-quad ICPMS (iCAP-TQ), Thermo Fisher Scientific, Germany). Briefly, the torch was warmed-up for 30 min in single-quad Kinetic energy discrimination (SQ-KED) mode with helium to remove the polyatomic nuclei interference and then autotuned in normal mode followed by advanced KED mode. Then the multi-element standard (#92091, Sigma Aldrich, USA) of different concentrations was run at the same settings to prepare the standard plot. Then sample blank was run followed by test samples. Quality controls (QC) of known concentrations were run after every 15-20 samples to ensure uniform signal intensity throughout the complete run. Data analysis was done using Qtegra software (Thermo Scientific, USA).

Statistical analysis: All data are presented as mean ± standard error of mean (SEM) values. Statistical analyses were performed using Origin 2020 and Microsoft Excel using unpaired two-tailed t test to identify group specific variations. Statistical differences were considered significant when $p<0.05$ at 95% confidence.

Results

Deferoxamine affects mycobacterial growth *in-vitro:* Iron chelation in *Mycobacteria* H37Rv by DFO leads to a compromised growth in a time dependent manner (Figure 1A). The growth kinetics of Mtb in the presence of DFO in 7H9 media was comparable to isoniazid treated groups (Figure 1A). In combination, DFO and isoniazid, also compromised Mtb growth kinetics (Figure 1A). At day 5 post inoculation, significant reduction in the Mtb survival in the presence of either DFO or isoniazid or both (Figure 1B, 1C) was observed. DFO treatment did not impact the total Fe in the culture filtrate (Figure 1D) but as expected DFO alone or in combination with isoniazid, significantly reduced Mtb intracellular Fe levels (Figure 1E). In

presence of DFO and isoniazid in combination, a significant reduction in intracellular Copper and Zinc levels was observed (Figure 1E). Interestingly, culture filtrate of DFO and isoniazid treated Mtb showed higher Copper levels and only in combination of DFO and isoniazid, Zinc levels were significantly low (Figure 1D). We analyzed the 3D structure of iron storage proteins of Mtb i.e. BfrA: Rv 1876 and BfrB: Rv3841 and observed that the biological units of both BfrA and B contain 24 submits arranged in a 432 molecular symmetry. Further, BfrA harbors 48 iron atoms and 12 heme moieties; whereas no iron atom has been incorporated into the 3D structure of BfrB. However, it is likely that BfrB would also contain 48 iron molecules in locations similar to those in BfrA (Figure 1E, F, G, H).

Iron supplementation leads to liver iron loading in C57BL/6 mice and higher tissue mycobacterial load: The methods adopted for iron supplementation are presented in Figure 2A and Supplementary Figure S1. Iron supplementation has negligible effect on the mice body weight during and after the course (data not shown). In the iron-supplemented mice, blood iron concentration and other elements like Selenium, Copper and Zinc were found to be similar to the control group **(Supplementary Figure S2)**. However, in the liver of iron supplemented mice group showed significantly higher iron levels compared to control (Figure 2B). Prussian blue staining of the liver samples of iron-supplemented groups also showed higher iron accumulation and distribution (Figure 2C). Levels of liver Zinc, Copper and Selenium in the iron-supplemented and control mice groups remain unaffected (data not shown). Muscle iron levels of iron supplemented mice didn't show major variations (Supplementary Figure S3). Gross pathology of lungs of the study groups showned differences (Supplementary Figure S4). The multiple tissue (lungs, liver, and spleen) mycobacterial burden was found to be significantly higher in iron supplemented mice groups at 15 days post infection compared to control (Figure 2D, 2E, 2F, Supplementary Figure S1B). Interestingly, the spleen and liver mycobacterial load was also higher at different time points post infection in iron supplemented

groups (Figure 2E, 2F, Supplementary Figure S1B). However, at 90 d.p.i. the liver mycobacterial load was higher in iron supplemented groups compared to control (Figure 2F, Supplementary Figure S1B).

Bactericidal activity of isoniazid and rifampicin is compromised in the iron supplemented group: Iron supplemented C57BL/6 mice showed higher tissue mycobacterial load at 15 days post infection. We aimed to understand the role of isoniazid and rifampicin treatment in iron supplemented condition (Figure 3A, Supplementary Figure S1B). Upon isoniazid and rifampicin treatment, liver iron levels of iron supplemented groups were significantly higher compared to control groups (Figure 3B). Prussian blue staining of liver samples obtained from iron supplemented mice groups showed higher iron accumulation till 75 days post treatment (Figure 3C, Supplementary Figure S1B). As expected, higher multiple tissue mycobacterial load was observed in iron supplemented groups compared to control at 15 days post infection (Figure 3C, 3D, 3E). However the mycobacterial clearance in the lungs and spleen of iron supplemented mice groups were delayed and took longer time (>30 days of treatment) to bring it to lower then the limit of detection (Figure 3C, 3D, Supplementary Figure S1B). Surprisingly the liver mycobacterial burden of the iron supplemented group was similar to the control groups. It seems that higher host iron levels compromise the anti-mycobacterial efficacy of the commonly used anti-TB drugs like isoniazid and rifampicin.

Iron chelation by deferoxamine (DFO) alone or as adjunct significantly reduced the tissue mycobacterial burden of C57BL/6 mice: Mtb infected C57BL/6 mice when received iron chelation agent like DFO without the anti-TB drugs significantly reduced the lung bacterial load within 30 days post treatment and continued up to 75 days post treatment compared to infected control (Figure 4A, 4B, Supplementary Figure S1B). Similarly, significantly lower liver mycobacterial load was observed in the DFO treated mice but remained similar in the spleen (Supplementary Figure S1B). The liver iron levels of DFO treated mice were

significantly low then control (Supplementary Figure S2). Interestingly, DFO treatment in Mtb infected iron supplemented mice group was ineffective in reducing tissue bacterial burden in the early time point (30 days post treatment) whereas a decreasing trend was observed in the lung and liver tissues. DFO showed anti-mycobacterial properties and may need longer treatment duration in iron supplemented groups to show its effectiveness. The lung mycobacterial burden in mice groups receiving DFO as adjunct to isoniazid and rifampicin showed similar mycobacterial load at 30 days post treatment with more mice have low bacterial load then the limit of detection then controls isoniazid and rifampicin treated group (Figure 4C, 4D, Supplementary Figure S1B). In iron supplemented groups, we observed mycobacterial colonies in 30 days of post treated groups (Supplementary Figure S1B).

Discussion: Several biological processes like cell wall synthesis, ATP synthesis, DNA coiling, transcription and translation in Mtb have been effectively used for developing drugs for its control in TB patients.[14] However limited studies have been attempted to understand how iron overloading condition affects Mtb growth and its influence on effectiveness of anti-TB agents as well as effect of iron limitation on survival ability of Mtb.[15,16] In this study, we attempted to generate evidence on how host iron plays critical role in Mtb survival and limiting it's availability using chemical agents like iron chelators may influence Mtb clearance in in-vitro and in vivo conditions.

Mtb cultured in 7H9 media supplemented with DFO showed high anti-bactericidal activity comparable to isoniazid. The anti-mycobacterial role of DFO in *in-vitro* condition observed in this study corroborates earlier reports.[7] DFO not only limits intracellular iron levels it also impacts Copper and Zinc levels. DFO also imports the expression of iron storage proteins (like BrfA/B) and oxidative stress genes (Figure 4E). DFO reported to increase glycolytic metabolism in Mtb infected hMDMs while taking care of the early innate immune response by increasing IL-1 and TNF-α both at transcript and protein levels (Figure 4E).[17] DFO reported to

reversibly inhibit DNA synthesis in human B and T lymphocytes with limited influence on the RNA and protein synthesis. In presence of equimolar $FeCl_3$ effect of DFO in these cells also reversed.[18]

Iron supplementation in C57BL/6 mice did not impact the body weight gain, corroborating earlier report in Sprague Dawley Rat Pup.[19] One of the primary functions of liver is to regulate iron homeostasis by detecting minor variations in the systemic iron requirements and excess iron gets accumulated in the liver.[20] Several regulatory mechanisms in the liver control the expression of the iron regulatory genes, storage capacity, and iron mobilization. Dysregulation of these functions result in iron imbalance, which is one of the primary causes of iron-related disorders.

Several reports have shown that iron supplementation in mice orally or parenterally supports the growth of non-tuberculous mycobacteria (NTM), however, the studies on Mtb are limited.[21] One of the preliminary studies by Kochan et al showed that iron supplementation in mice significantly increased the Mtb burden in spleen and lung tissues.[22] We looked at the impact of host iron status on Mtb survival and growth *in-vivo*. And observed that iron supplementation using ferric carboxymaltose intravenously favors mycobacterial growth in lung, liver, and spleens up to a few weeks post supplementation, but that effect diminishes in a couple of months after stopping supplementation.

Limiting iron by treating Mtb infected mice with DFO significantly reduced liver iron levels and tissue mycobacterial burden compared to the infected control group. Interestingly, DFO has limited effect in the iron-supplemented mice till 75 days of treatment, however, there was a declining trend after 60 days of treatment. This indicates that either longer treatment duration or different dose of DFO might control Mtb in an iron overloaded condition which needs additional studies. The liver iron levels in iron overloaded C57BL/6 mice showed significant decline upon DFO treatment.

We further evaluated the effect of DFO as an adjunct to anti-TB drugs with INH and RIF. There were no noticeable differences in the Mtb colonies between DFO with or without isoniazid and rifampicin treated animals. DFO as an adjunct to existing TB drugs may reduce the lengthy anti-TB treatment, however, it needs appropriate clinical studies for further validation. Whether DFO as an adjunct might also reduce the existing TB drug dose might be an interesting avenue to explore.

Our findings highlight the role of DFO as an adjunct therapeutic agent (DFO) for treating TB and provides new insights into manipulating host iron metabolism which may reduce the treatment duration. Iron chelation in hosts could be useful as a host-directed therapies (HDTs) and needs additional validation to understand its role in limiting drug resistance development, if any! Particular focus on the toxicity of DFO treatment needs to be taken care and in cellular system it showed that equivalent amount of $FeCl_3$ introduction negates its function.[19] DFO is an FDA approved drug, have pro-inflammatory properties and used for hemochromatosis in humans.[23] Here, we demonstrated the role of DFO as adjunct therapeutics to reduce Mtb burden by limiting iron availability in the C57BL/6 mice.

We hypothesized that the combined effects of DFO with first-line anti-TB drugs may have higher bactericidal effects and may reduce the treatment duration. Cahill et al have shown that in BCG infected primary hMDMs treated with DFO showed a higher bactericidal effect of bedaquiline.[7] Additive effect of DFO with the second line anti-TB drugs need additional studies to monitor their effectiveness in clearing drug resistant Mtb isolates. Limiting other critical trace elements like Cu, Zn and Mg that are important for Mtb survival and growth might also be useful target for treating TB.[24,25,26] Role of gene polymorphisms of NRAMP1, HFE (haemochromatosis), Hp and β2m genes that contributes for TB susceptibility may facilitate to identify the populations that may get benefit from iron chelation therapy. [4,27]

Currently there is no effective vaccine available for TB and drug resistance cases have been on the rise in recent times. Adding therapeutic agents that increase the effectiveness of current chemotherapeutics will significantly reduce TB associated morbidity and mortality. Several FDA-approved drugs have received attention as viable adjunctive HDTs for use as combination therapy with the existing TB drugs. Based on our and others findings, it is evident that DFO administration increases host immunity to control *Mtb* and has a potential as agent for host directed adjunct therapy. It seems to effectively combat *Mtb* and such new therapeutic interventions targeting host or pathogen iron metabolism like iron chelation will add significance.

Online supplemental material: Four supplemental figures are available in the Supplemental file.

Acknowledgments: We acknowledge the Department of Biotechnology (DBT), Government of India for supporting activities through research grants and supporting Tuberculosis Aerosol Challenge Facility at ICGEB and the ICGEB New Delhi for providing access to ICP-MS facility and core support to RKN. Sandeep R. Kaushik received a Senior Research Fellowship from the DBT, Sukanya Sahu received support from the Council of Scientific and Industrial Research (CSIR) New Delhi and Nidhi Yadav received . All hospital staff involved in subject recruitment, testing, and classification are highly acknowledged. We thank Ms Shweta Chaudhury for helping to prepare the schematics using BioRender and Ms Mothe Sravya for helping in manuscript preparation.

Authorship Contributions: SRK, SS, AKM, NY, AS carried out all the laboratory profiling experiments; SK and BB took care of the Mtb protein structure study; funds for this work was

generated by RKN; SRK and RKN wrote the first draft of the manuscript and revised it, incorporating the comments of all coauthors.

Disclosure of Conflicts of Interest

All authors declare no conflict of interest.

References

1. https://www.cdc.gov/tb/topic/basics/default.htm (accessed on 31/05/2023)

2.Revised National Tuberculosis Control Programme (RNTCP) https://tbcindia.gov.in/WriteReadData/NSP Draft 20.02.2017 1.pdf (accessed on 31/05/2023)

3. Hawn TR, Matheson AI, Maley SN, Vandal O. Host-directed therapeutics for tuberculosis: can we harness the host? Microbiol Mol Biol Rev. 2013 Dec;77(4):608-27.

4. Boelaert JR, Vandecasteele SJ, Appelberg R, Gordeuk VR. The effect of the host's iron status on tuberculosis. J Infect Dis. 2007 Jun 15;195(12):1745-53.

5. Phelan JJ, Basdeo SA, Tazoll SC, McGivern S, Saborido JR, Keane J. Modulating Iron for Metabolic Support of TB Host Defense. Front Immunol. 2018 Oct 15;9:2296.

6. Lounis N, Maslo C, Boelaert JR, Bonnafous P, Trnffot-Pernot C, Baohong J, Grosset J. Impact of iron loading and iron chelation on murine tuberculosis. Clinical Microbiology and Infection. 199; 5 (11):687-692.

7. Cahill C, O'Connell F, Gogan KM, Cox DJ, Basdeo SA, O'Sullivan J, Gordon SV, Keane J, Phelan JJ. The Iron Chelator Desferrioxamine Increases the Efficacy of Bedaquiline in Primary Human Macrophages Infected with BCG. Int J Mol Sci. 2021 Mar 13;22(6):2938.

8. Schaible UE, Collins HL, Priem F, Kaufmann SH. Correction of the iron overload defect in beta-2-microglobulin knockout mice by lactoferrin abolishes their increased susceptibility to tuberculosis. J Exp Med. 2002 Dec 2;196(11):1507-13.

9. Pal R, Hameed S, Fatima Z. Iron Deprivation Affects Drug Susceptibilities of Mycobacteria Targeting Membrane Integrity. J Pathog. 2015;2015:938523.

10. McMath LM, Contreras H, Owens CP, Goulding CW. The structural characterization of bacterioferritin, BfrA, from Mycobacterium tuberculosis. J. Porphyrins Phthalocyanines 2013; 17, 229–239.

11. Khare G, Gupta V, Nangpal P, Gupta RK, Sauter NK, Tyagi AK. Ferritin structure from Mycobacterium tuberculosis: comparative study with homologues identifies extended C-terminus involved in ferroxidase activity. PLoS One. 2011 Apr 8;6(4):e18570.

12. wwPDB consortium. Protein Data Bank: the single global archive for 3D macromolecular structure data. Nucleic Acids Res. 2019 Jan 8;47(D1):D520-D528.

13. DeLano W L. The PyMOL molecular graphics system. http://www. pymol. org (2002).

14. Horsburgh CR, Barry E, Lange C. Treatment of Tuberculosis. N Engl J Med 2015; 373:2149-2160

15. Theriault ME, Pisu D, Wilburn KM, Lê-Bury G, MacNamara CW, Michael Petrassi H, Love M, Rock JM, VanderVen BC, Russell DG. Iron limitation in M. tuberculosis has broad impact on central carbon metabolism. Commun Biol. 2022 Jul 9;5(1):685.

16. Rodriguez GM. Control of iron metabolism in Mycobacterium tuberculosis. Trends Microbiol. 2006 Jul;14(7):320-7.

18. Phelan JJ, McQuaid K, Kenny C, Gogan KM, Cox DJ, Basdeo SA, O'Leary S, Tazoll SC, Ó Maoldomhnaigh C, O'Sullivan MP, O'Neill LA, O'Sullivan MJ, Keane J. Desferrioxamine Supports Metabolic Function in Primary Human Macrophages Infected With Mycobacterium tuberculosis. Front Immunol. 2020 May 13;11:836.

19. Lederman HM, Cohen A, Lee JW, Freedman MH, Gelfand EW. Deferoxamine: a reversible S-phase inhibitor of human lymphocyte proliferation. Blood. 1984 Sep;64(3):748-53.

20. McMillen S, Lönnerdal B. Postnatal Iron Supplementation with Ferrous Sulfate vs. Ferrous Bis-Glycinate Chelate: Effects on Iron Metabolism, Growth, and Central Nervous System Development in Sprague Dawley Rat Pups. Nutrients. 2021 Apr 22;13(5):1406.

21. Anderson ER, Shah YM. Iron homeostasis in the liver. Compr Physiol. 2013 Jan;3(1):315-30.

22. Agoro R, Mura C. Iron Supplementation Therapy, A Friend and Foe of Mycobacterial Infections? Pharmaceuticals (Basel). 2019 May 17;12(2):75.

23. Kochan I. The role of iron in bacterial infections, with special consideration of host-tubercle bacillus interaction. Curr Top Microbiol Immunol. 1973;60:1-30.

24. Parker JB, Griffin MF, Downer MA, Akras D, Berry CE, Cotterell AC, Gurtner GC, Longaker MT, Wan DC. Chelating the valley of death: Deferoxamine's path from bench to wound clinic. Front Med (Lausanne). 2023 Feb 15;10:1015711.

26. Mehdiratta K, Singh S, Sharma S, Bhosale RS, Choudhury R, Masal DP, Manocha A, Dhamale BD, Khan N, Asokachandran V, Sharma P, Ikeh M, Brown AC, Parish T, Ojha AK, Michael JS, Faruq M, Medigeshi GR, Mohanty D, Reddy DS, Natarajan VT, Kamat SS, Gokhale RS. Kupyaphores are zinc homeostatic metallophores required for colonization of Mycobacterium tuberculosis. Proc Natl Acad Sci U S A. 2022 Feb 22;119(8):e2110293119.

27. Piddington DL, Kashkouli A, Buchmeier NA. Growth of Mycobacterium tuberculosis in a defined medium is very restricted by acid pH and Mg(2+) levels. Infect Immun. 2000 Aug;68(8):4518-22.

28. Dow A, Sule P, O'Donnell TJ, Burger A, Mattila JT, Antonio B, Vergara K, Marcantonio E, Adams LG, James N, Williams PG, Cirillo JD, Prisic S. Zinc limitation triggers anticipatory adaptations in Mycobacterium tuberculosis. PLoS Pathog. 2021 May 14;17(5):e1009570.

29. Li X, Yang Y, Zhou F, Zhang Y, Lu H, Jin Q, Gao L. SLC11A1 (NRAMP1) polymorphisms and tuberculosis susceptibility: updated systematic review and meta-analysis. PLoS One. 2011 Jan 25;6(1):e15831.

Figure Legends

Figure 1: Deferoxamine (DFO) chelates iron and show anti-mycobacterial effect in the in-vitro culture. **A.** Growth kinetics of *Mycobacterium tuberculosis* H37Rv strain in absence and presence of different drugs (DFO, isoniazid: INH, DFO+INH) and in control. **B.** Absorbance of mycobacterial growth at 5th day post drug treatment and control showed significant bactericidal effect of the drugs alone or in combination. **C.** Survived Mycobacteria cultures on day 5 post drug treated conditions and control as observed in colony forming unit (CFU) assay. **D.** Elemental levels of the culture filtrate at 5th day post drug treated Mycobacterial culture quantified using ICP-MS. **E.** Intracellular elemental levels in Drug treated and control Mycobacterial culture at 5th day post treatment. Cartoon representation of the quaternary structure of the biological unit (24-mer assembly) of Bacterioferritin A (BfrA) (PDB ID: 3QB9, McMath et al., 2013). The biological unit exhibits a 432 molecular symmetry. **F and G** panels represent the arrangement of subunits with 4 and 3-fold rotational symmetry perpendicular to the plane of the paper, respectively. The assembly contains 48 iron atoms (shown as red spheres) and 12 heme moieties (shown as green stick-model), **H and I.** Cartoon representation of the quaternary structure of the biological unit of BfrB (PDB ID: 3QD8, Khare et al., 2011). The arrangement of the 24 subunits of BfrB is same as that in BfrA. No iron has been modelled into this structure. ns: not significant; *: $p<0.05$; **: $p<0.01$; ***: $p<0.001$; ****:$p<0.005$ at 95% confidence interval.

Figure 2: Iron loading condition increases tissue Mycobacterial burden in C57BL/6 mice. **A.** Schematic presentation of the method used to create iron loading condition for subsequent Mycobacterial infection experiment. **B.** Liver iron levels, as estimated using ICP-MS, in iron loaded and control mice groups. **C.** Prussian Staining of liver tissues indicates high iron accumulation. Mycobacterial load in the (**D**) lungs, (**E**) spleen and (**F**) liver of the *Mycobacteria tuberculosis* H37Rv infected C57BL/6 mice. n = 5/group/time points; i.v.: intra-

venous injection; d.p.i./dpi: days post infection; CFU: colony forming units; p-values at 95% confidence interval.

Figure 3: Iron loading in C57BL/6 mice compromises bactericidal activity of isoniazid and rifampicin and takes longer time for tissue Mycobacterial burden. A. Schematic presentation of the method used to create iron loading condition, Mycobacterial infection and treatment (with isoniazid: INH and rifampicin: RIF) experiment. **B.** Liver iron levels, as estimated using ICP-MS, in iron loaded and control mice groups. **C.** Prussian Staining of liver tissues indicates high iron accumulation in iron loaded mice and did not change significantly upon drug treatment. Mycobacterial load in the lungs (**D**), spleen (**E**) and liver (**F**) of the *Mycobacteria tuberculosis* H37Rv infected C57BL/6 mice. n = 5/group/time points; i.v.: intra-venous injection; dpi: days post infection; CFU: colony forming units; p-values at 95% confidence interval.

Figure 4: Deferoxamine (DFO) alone or adjunct to anti-tuberculosis drugs (isoniazid and rifampicin) aids in Mycobacterial clearance in C57BL/6 mice. A. Schematic presentation of the method used to infect C57BL/6 mice with Mycobacterial tuberculosis H37Rv strain and treated using DFO. **B.** Lung mycobacterial load of control and DFO treated C57BL/6 mice. **C.** Schematic showing the infection and treatment using isoniazid (INH) and rifampicin (RIF) with or without DFO. **D.** Lung mycobacterial load of the *Mycobacteria tuberculosis* H37Rv infected C57BL/6 mice receiving isoniazid and rifampicin with or without DFO. **E.** Effect of DFO on Mycobacterium and Macrophages infected with Mycobacteria. n = 5/group/time points; dpi: days post infection; CFU: colony forming unit; i.p.: intra-peritonium introduction; p-values at 95% confidence interval.

Figure 1

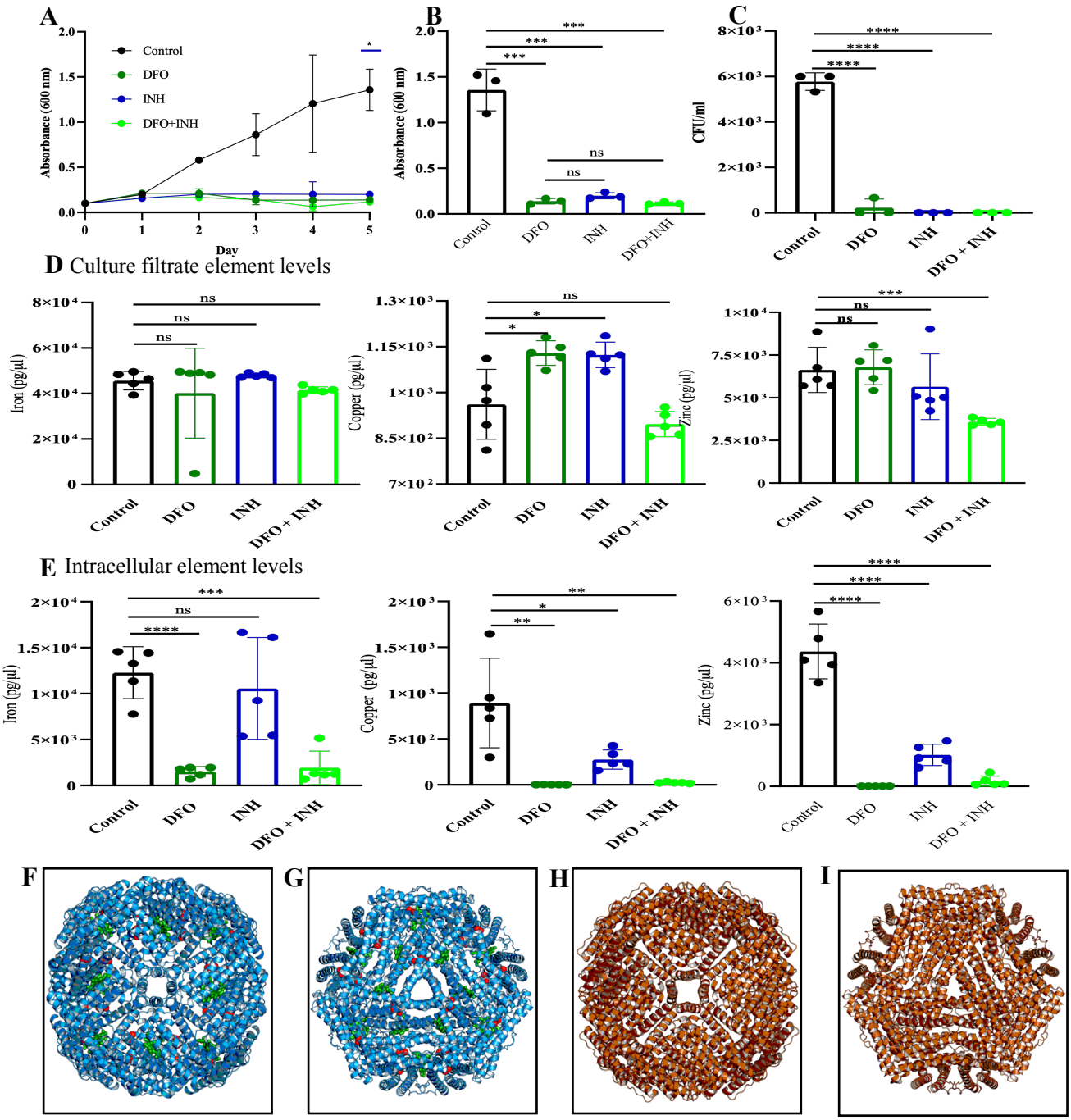
A
Control
DFO
INH
DFO+INH
Absorbance (600 nm)
Day
B
Absorbance (600 nm)
Control
DFO
INH
DFO+INH
C
CFU/ml
Control
DFO
INH
DFO + INH
D Culture filtrate element levels
Iron (pg/µl)
Copper (pg/µl)
Zinc (pg/µl)
E Intracellular element levels
Iron (pg/µl)
Copper (pg/µl)
Zinc (pg/µl)
F
G
H
I

Figure 2

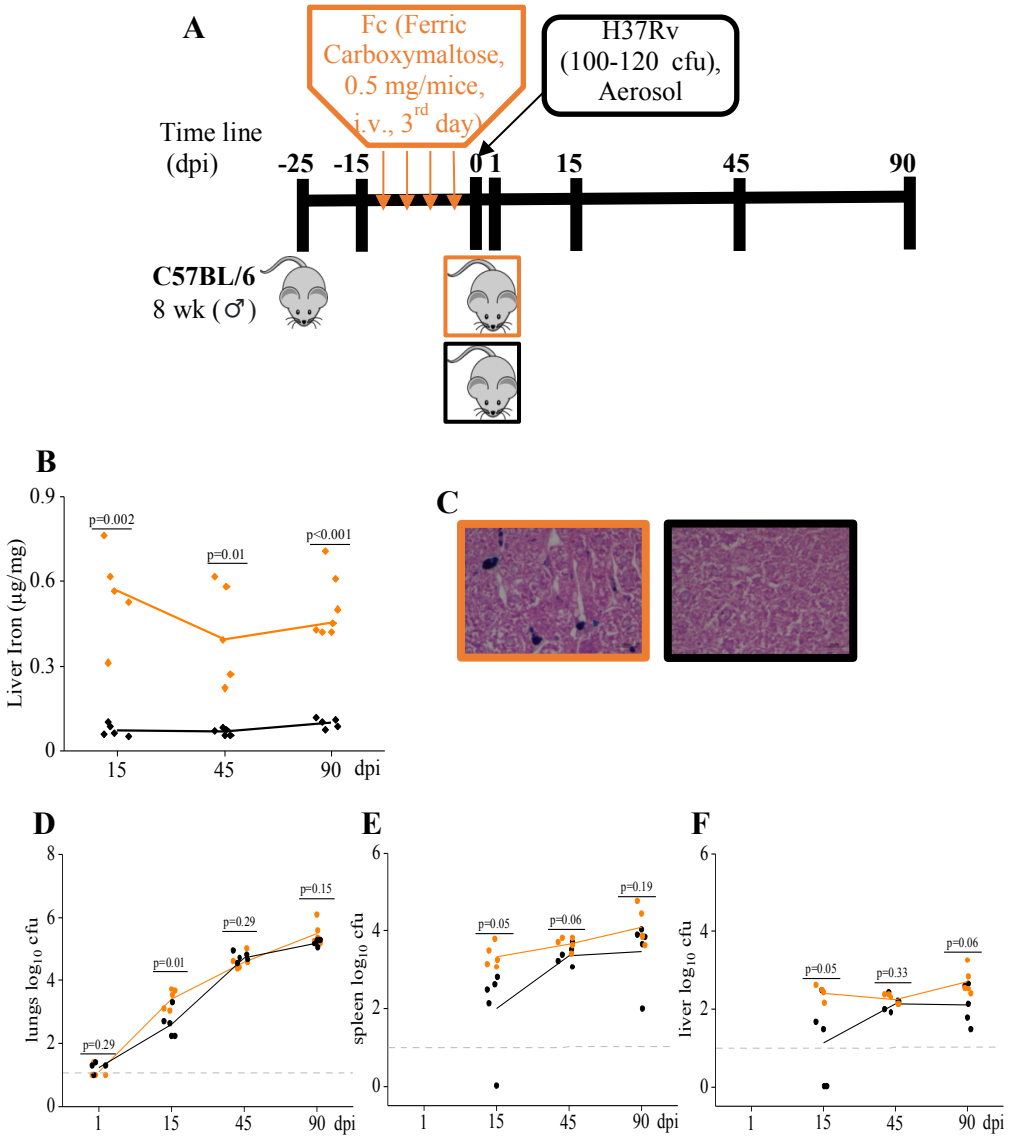
A
Fc (Ferric Carboxymaltose, 0.5 mg/mice, i.v., 3rd day)
H37Rv (100-120 cfu), Aerosol
Time line (dpi)
-25 -15 0 1 15 45 90
C57BL/6
8 wk (♂)
B
Liver Iron (µg/mg)
p=0.002
p=0.01
p<0.001
15 45 90 dpi
C
D
lungs log10 cfu
p=0.29
p=0.01
p=0.29
p=0.15
1 15 45 90 dpi
E
spleen log10 cfu
p=0.05
p=0.06
p=0.19
1 15 45 90 dpi
F
liver log10 cfu
p=0.05
p=0.33
p=0.06
1 15 45 90 dpi

Figure 3

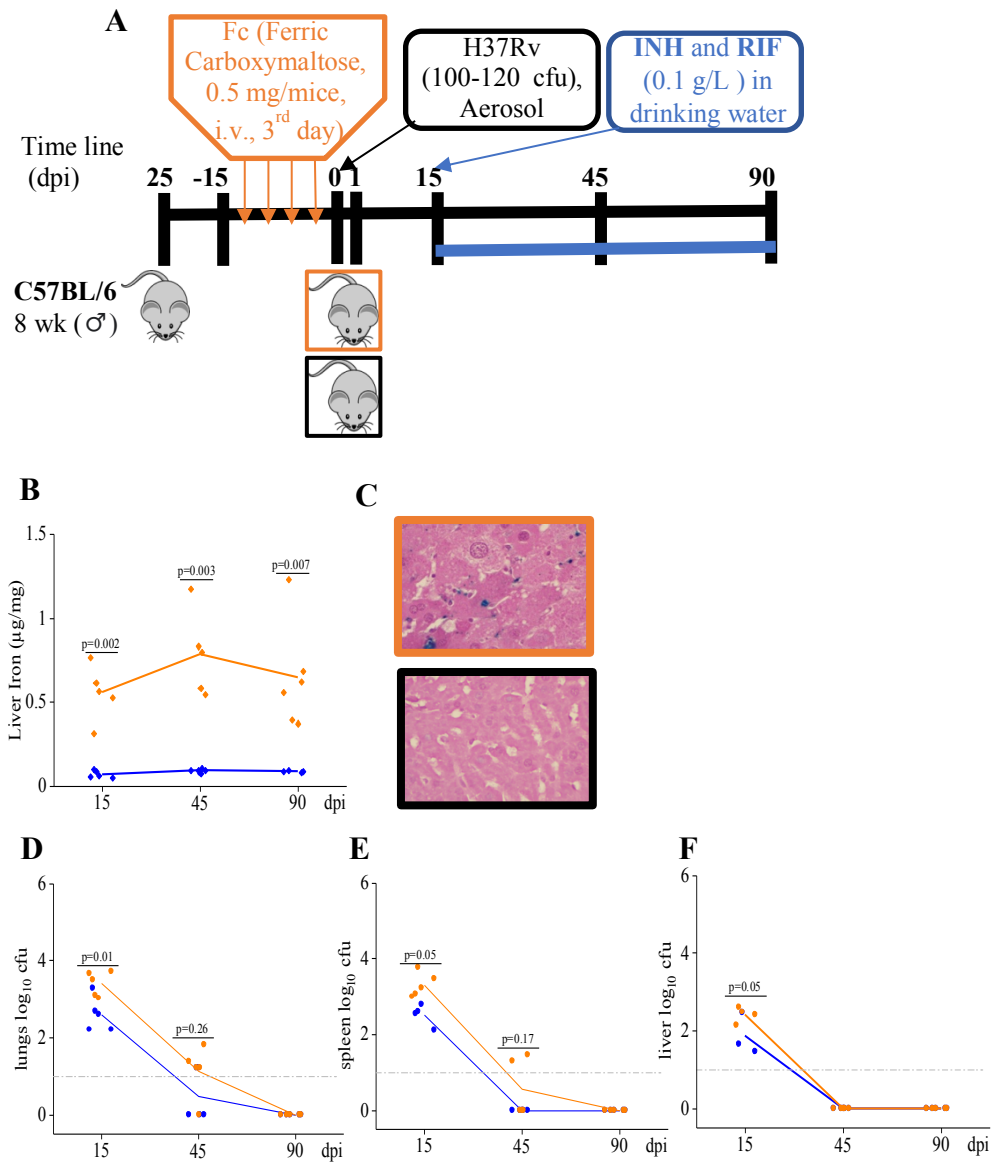
A
Fc (Ferric Carboxymaltose, 0.5 mg/mice, i.v., 3rd day)
H37Rv (100-120 cfu), Aerosol
INH and RIF (0.1 g/L) in drinking water
Time line (dpi)
25
-15
0
1
15
45
90
C57BL/6
8 wk (♂)
B
Liver Iron (µg/mg)
p=0.002
p=0.003
p=0.007
dpi
C
D
lungs log10 cfu
p=0.01
p=0.26
E
spleen log10 cfu
p=0.05
p=0.17
F
liver log10 cfu
p=0.05

Figure 4

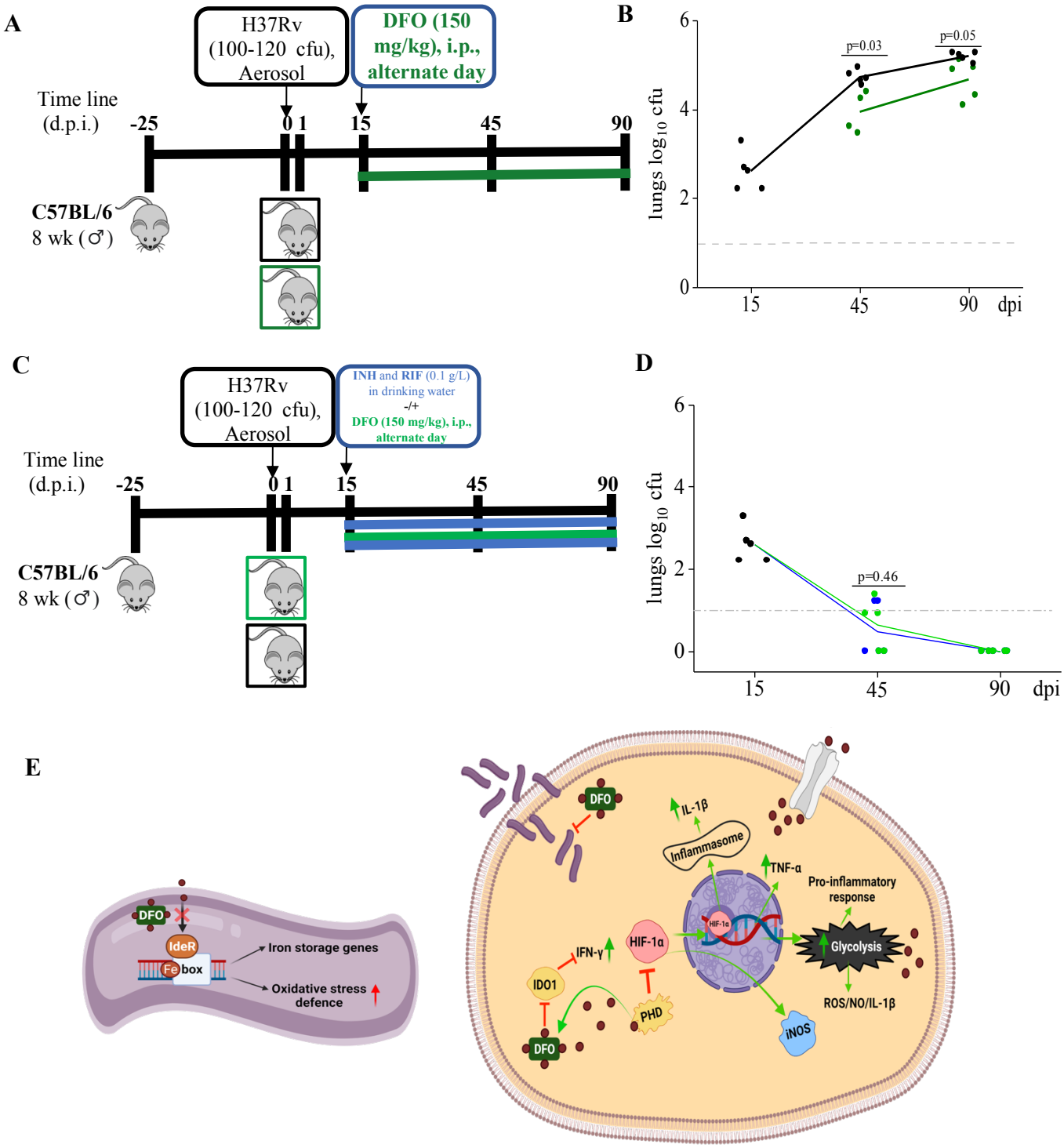
A
H37Rv (100-120 cfu), Aerosol
DFO (150 mg/kg), i.p., alternate day
Time line (d.p.i.)
-25
0 1
15
45
90
C57BL/6 8 wk (♂)
B
lungs log10 cfu
p=0.03
p=0.05
dpi
C
INH and RIF (0.1 g/L) in drinking water -/+ DFO (150 mg/kg), i.p., alternate day
D
p=0.46
E
DFO
IdeR
Fe box
Iron storage genes
Oxidative stress defence
IL-1β
Inflammasome
TNF-α
Pro-inflammatory response
HIF-1α
Glycolysis
IFN-γ
IDO1
PHD
ROS/NO/IL-1β
iNOS